RAPID COMMUNICATIONS

PHYSICAL REVIEW E VOLUME 52, NUMBER 6 DECEMBER 1995

# Critical dynamics of contact-line motion

Suman Kumar, Daniel H. Reich, and Mark O. Robbins
*Department of Physics and Astronomy, The Johns Hopkins University, Baltimore, Maryland 21218*
(Received 21 July 1995)

The velocity $V$ of the contact line where a fluid interface intersects the wall of a tube depends on the applied capillary pressure $P_{cap}$. We have used sensitive ac differential-pressure measurements, to study the scaling of $P_{cap}$ with $V$ for water-alkane interfaces in tubes that have disordered surfaces. Our results are consistent with a critical depinning transition. The derivative $dP_{cap}/dV \sim V^x$ over two decades in velocity in the critical regime near $V=0$. We find similar critical exponents for water-hexadecane, $x=-0.77(5)$, and water-decane systems, $x=-0.81(5)$. The exponent does not depend on the direction of flow or on the degree of surface roughness on the tube walls.

PACS number(s): 68.10.−m, 68.45.−v

The spreading of liquids on solid surfaces is governed by the dynamics of the three-phase, or contact, line where a liquid-liquid or liquid-vapor interface intersects a solid wall. An understanding of contact-line motion is relevant to many industrial processes such as the application of coatings and lubricants, and oil recovery from porous media [1]. A stationary fluid interface and a smooth homogeneous surface intersect at a unique static contact angle $\theta_s$ which is determined by the balance of interfacial tensions between the three media. When these forces become unbalanced, the interface moves and there is a new "dynamic" contact angle $\theta$ that reflects the influence of viscous dissipation. Hydrodynamic theory [2] and simulations [3] show that $(\cos\theta - \cos\theta_s)$ varies linearly with interface velocity on ideal surfaces. However, chemical heterogeneities and surface roughness lead to qualitatively different behavior on real surfaces. One of the most prominent effects is contact angle hysteresis — a finite range of static contact angles due to pinning of the contact line in one of the many metastable states produced by disorder on the surface [4,5].

It has been suggested that the onset of contact-line motion on a disordered surface is a critical depinning transition [5,6]. If so, this system belongs to a broad class of problems involving collective transport in an environment with quenched (static) disorder. Examples include charge density wave conduction [7], flux vortex motion in type II superconductors [8], fluid invasion in porous media [9], and magnetic domain wall motion [10,11]. Theoretical arguments [7,9,12] and simulations [10,13,14] indicate that such systems undergo a critical transition from a stationary to a moving state at a threshold value $F_t$ of the applied force. For $F > F_t$, the velocity $V$ scales as

$$V \sim (F - F_t)^{\zeta} \tag{1}$$

and motion occurs through a sequence of "avalanches" whose maximum size diverges with the correlation length: $\xi \sim (F - F_t)^{-\nu}$. However, experimental verification of this predicted critical behavior has proved difficult [15].

In the case of contact-line motion, the applied force is the capillary pressure $P_{cap}$ across the interface. In a capillary of radius $R$, and at low velocities [16], $P_{cap}$ is directly related to $\cos\theta$ by

$$P_{cap} = \frac{2\gamma}{R}\cos\theta, \tag{2}$$

where $\gamma$ is the interfacial tension of the fluid interface. Recent experiments on moving interfaces show that $\cos\theta$ varies nonlinearly with velocity, but there is no consensus on the critical exponent, or even that $\cos\theta$ follows a power law [17–20].

In this paper we present measurements of the velocity dependence of $\cos\theta$ for pairs of immiscible fluids in capillaries. We use an experimental technique pioneered by Stokes *et al.* [18] that measures $d\cos\theta/dV$ by adding an oscillatory velocity $V_{ac}$ to the mean dc velocity $V$. Our apparatus can measure the interface response at velocities two orders of magnitude closer to the critical point than was previously possible. Moreover, we do not need to match the viscosity of the two fluids and can therefore use pure fluids instead of mixtures. We observe power-law scaling consistent with a critical depinning transition over two decades in $V$, $d\cos\theta/dV \sim V^x$ where $x = (1/\zeta) - 1$. For the cases studied, $x$ was independent of the fluids used, the direction of flow and surface roughness.

The experimental apparatus is sketched in Fig. 1. The total pressure drop is set by varying the height of the water reservoir. A high-hydrodynamic-impedance capillary $T_1$ in series with the sample tube $T_2$ ensures a constant $V$ for a given height. A speaker, driven with a signal generator, is coupled to the fluids through a flexible membrane to generate an ac flow $V_{ac}$ at frequency $\omega$ (0.025 to 1 Hz). $V_{ac}$ is determined from the viscous pressure across a third tube $T_3$. Piezoelectric pressure sensors (Omega PX-170) $S_1$ and $S_2$ are placed at either end of the sample tube. The sensor outputs $P_1$ and $P_2$ are digitized with a HP3458A multimeter, and the ac response is extracted by digital lock-in techniques [21].

To measure $V$, the capacitance of a pair of semicylindrical copper plates placed along the length of the sample capillary is monitored with a Keithley 590CV capacitance meter. The dielectric contrast between the fluids ($\epsilon_{water} \sim 80$, $\epsilon_{alkane} \sim 2$) produces a linear capacitance change of 20 fF per cm of interface motion. The slope of the measured capacitance with time yields $V$ within an uncertainty of 1%. The capacitance measurement is also used to ensure that

 

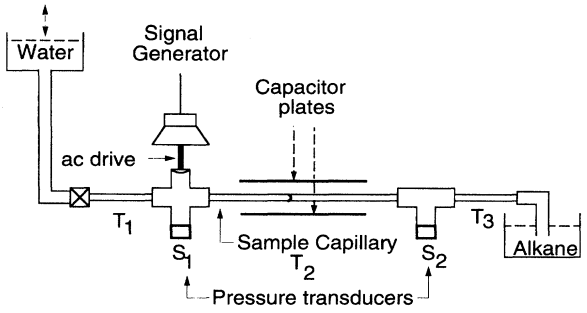


FIG. 1. Schematic of the experimental setup. The fluid-fluid interface is in the sample tube $T_2$. A pressure gradient is set by varying the height of the water reservoir. The high-hydraulic-impedance tube $T_1$ ensures constant dc velocity $V$. The ac drive generates $V_{ac}$. The transducer $S_2$ measures $V_{ac}$ by measuring the ac pressure drop across $T_3$, while the difference in the outputs of $S_1$ and $S_2$ contains information about the dynamics of the interface. The capacitor plates are used to measure $V$.

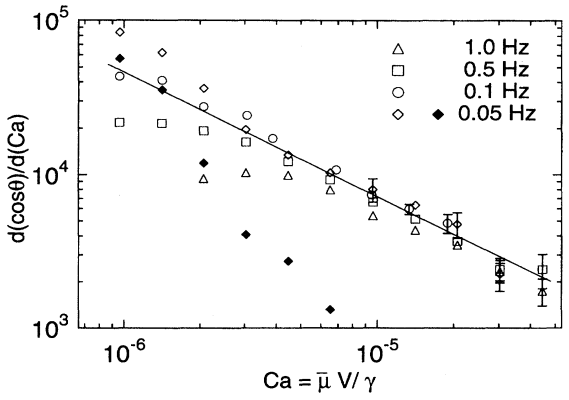


FIG. 2. Frequency dependence of the in-phase response (open symbols) of a water-decane interface with $\mu V_{ac}/\gamma = 2.5\times10^{-6}$. The out-of-phase response at 0.05 Hz is also indicated (closed symbols). The straight line shows the power-law fit for water-decane from Fig. 4.

$d\cos\theta/dV$ is measured over the same 20 cm section of $T_2$ at each $V$. This eliminates possible systematic effects due to variations in heterogeneity, viscosity, and tube diameter.

The sample capillaries were precision-bore Pyrex tubes of radius $R=0.5$ mm ($\pm2.5$ $\mu$m) and length $L=30$ cm. For $T_1$, $R=0.1$ mm and $L=15$ cm. Two different tubes were used for $T_3$ ($R$ = 0.254 mm, $L$ = 12.0 cm and $R$ = 0.381 mm, $L$ = 6.65 cm) to ensure that $P_2$ and $P_1-P_2$ had comparable magnitudes over the entire range of $V_{ac}$ and $V$. All tubes used in the experiments were first washed with ether, then in near-saturated alkaline solutions (KOH or NaOH), and finally ultrasonically cleaned in deionized distilled water. The surface tensions of the sample fluids were measured after the experiments to ensure that there was no contamination by surfactants. To explore the effects of surface roughness, measurements were also done in a sample capillary that was etched with a 30% aqueous solution of hydrofluoric acid for 4 min at room temperature.

We have measured the response of water-hexadecane ($\gamma=32.6$ dyn/cm) and water-decane ($\gamma=41$ dyn/cm) interfaces over the range $2\times10^{-3}$ cm/s$<V<2.3\times10^{-1}$ cm/s. We present results for the dimensionless derivative $d\cos\theta/d\mathrm{Ca}$, where the capillary number $\mathrm{Ca}\equiv\bar{\mu}V/\gamma$ and $\bar{\mu}$ is the mean viscosity of the two fluids. For the above velocity range, $5\times10^{-7}<\mathrm{Ca}<1.5\times10^{-4}$.

A fluid of viscosity $\mu$ moving with mean velocity $V$ in a capillary produces a viscous pressure drop $P_{visc}=8\mu VL/R^2$ at low $\omega$. The viscous contribution to the ac pressure across $T_2$, $P^{12}=P_1-P_2$, varies with interface position if the fluids have different viscosities. The water-decane pair is naturally viscosity matched at room temperature ($\mu_{H_2O}=1.0$ cP, $\mu_{decane}=$ 0.9 cP) while hexadecane has a higher viscosity ($\mu_{hex}$ = 3.3 cP). The mean viscous pressure is determined from measurements with the interface displaced past each end of $T_2$. In the limits of small $\omega$ and $V_{ac}$ discussed below, the average of the total ac response $P_{ac}^{12}$ over a length of $T_2$ satisfies

$$P_{ac}^{12}=\frac{8\bar{\mu}L}{R^2}V_{ac}+\frac{2\gamma}{R}\frac{d\cos\theta}{dV}V_{ac}+O(V_{ac}^3), \tag{3}$$

where the second term on the right gives the capillary pressure we are interested in. We extract $d\cos\theta/d\mathrm{Ca}$ by subtracting the viscous term from the in-phase component of $P_{ac}^{12}/V_{ac}$ and multiplying by $R/2\bar{\mu}$.

Equation (3) is valid in the low frequency limit where $P_{ac}$ and $V_{ac}$ are in phase. As shown for the water-decane system in Fig. 2, for a given $\omega$ the in-phase response rolls over at low $V$. A corresponding increase is observed in the out-of-phase component. Both features move to lower $V$ as $\omega$ decreases. All measurements reported below were made at a frequency where the out-of-phase component was negligible.

Previous calculations predicted that the response should be in phase when $\omega$ is much less than the characteristic frequency for the curvature of the interface to adapt to changes in the contact angle [16,18,22]:

$$\omega_0=\frac{\gamma}{\mu R}\left[\frac{d\cos\theta}{d\mathrm{Ca}}\right]^{-1}\sin\theta(1+\sin\theta)^2, \tag{4}$$

where $d\cos\theta/d\mathrm{Ca}$ is evaluated in the limit $\omega\to0$. The value of $\omega_0$ decreases with $V$ due to the rise in $d\cos\theta/d\mathrm{Ca}$, in qualitative agreement with the decrease in rollover frequency seen in Fig. 2. However, the observed rollover frequency is consistently lower than $\omega_0$. For example, $\omega_0/2\pi\sim1$ Hz at $\mathrm{Ca}=10^{-6}$ and 6.5 Hz at $\mathrm{Ca}=10^{-5}$, yet the in-phase component is sharply depressed at frequencies much lower than these values. The expression for $\omega_0$ is based on the assumption that the interface adopts the appropriate dynamic contact angle $\theta$ for the instantaneous velocity. Our data indicate that there is a lower frequency related to the relaxation of $\theta$ which may be related to the critical behavior. Fermigier and Jennfer [17] found that $\theta$ stabilized after the contact line advanced by a distance of about $R$. This would imply a

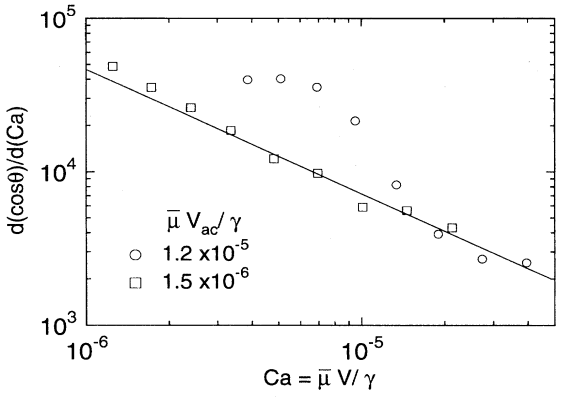


FIG. 3. The amplitude dependence of the in-phase response at fixed frequency (0.1 Hz) and the indicated ac capillary numbers. The straight line shows the power-law fit for water-decane from Fig. 4.

characteristic frequency of $Ca\gamma/\mu R$ or about 0.08 Hz at $Ca=10^{-6}$ which is more in-line with our measurements.

The data in Fig. 2 are also affected by the increase in $V_{ac}/V$, as $V$ is decreased at fixed $V_{ac}$. When $V_{ac}/V>0.5$ the nonlinear terms in $V_{ac}$ in Eq. (3) become important. Figure 3 shows their effect for two different $V_{ac}$ at $\omega=0.1$ Hz. The data rise above the linear response curve obtained at low $V_{ac}/V$ (solid line) before rolling over due to the frequency effects described above. All data presented below were taken in the limit of $V_{ac}/V\leq 1/3$, to ensure that they accurately reflect $d\cos\theta/d\mathrm{Ca}$.

Figure 4 shows $d\cos\theta/d\mathrm{Ca}$ for water-decane and water-hexadecane interfaces. Data for both water-alkane pairs are described by the power law $d\cos\theta/d\mathrm{Ca}=B(\mathrm{Ca})^x$. Fits for

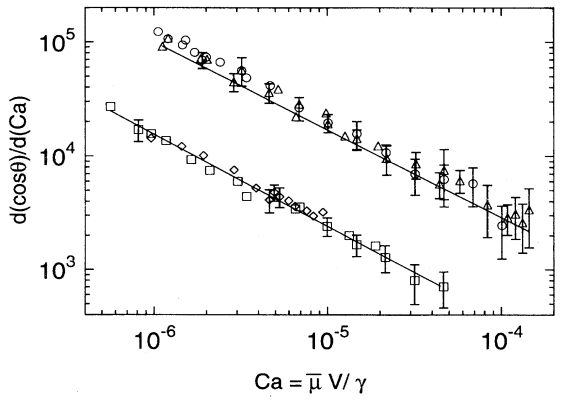


FIG. 4. Values of $d\cos\theta/d\mathrm{Ca}$ obtained from the averaged in-phase response in the low $V_{ac}$ and low frequency limits. Data for water-decane in unetched tubes with water advancing (squares) and receding (diamonds) are divided by 3 to prevent overlap with data for water displacing hexadecane in unetched (triangles) and etched (circles) tubes. The straight lines are fits to the data shown by squares and triangles and have slope $-0.81$ and $-0.77$, respectively. Error bars are shown when uncertainties are larger than the symbol size.

water advancing (solid lines) give $B=0.7(2)$ and $x=-0.81(5)$ for water-decane, and $B=1.1(3)$ and $x=-0.77(5)$ for water-hexadecane. Consistent data were obtained with several Pyrex tubes of similar diameter, with the flow direction reversed (diamonds), and also for a chemically etched tube with increased surface roughness (circles). The etched tube exhibits greater contact angle hysteresis than the unetched tube, as described below, but fits to the data in Fig. 4 give a nearly identical value of $x$ for water-hexadecane: $x=-0.81(5)$ and $B=1.6(3)$. Taken together, these results suggest a universal value of $x=-0.80(3)$, which implies $1/\zeta=0.20(3)$.

The above power-law scaling extends to the lowest and highest velocities at which we can measure $d\cos\theta/d\mathrm{Ca}$. Two factors determine the maximum velocity. The first is the size of the viscous background. The second is that the interface begins to leave behind thin patches of the displaced fluid when $|\cos\theta|>0.9$. With the water receding, $|\cos\theta|$ starts at a large value, and the data become irreproducible for $|\mathrm{Ca}|>10^{-5}$ in the unetched tube. The contact angle hysteresis $\Delta\cos\theta$ was measured by increasing the reservoir height in a sequence of small steps and determining the pressures at which $|V|$ differed from zero. By waiting for about 12 h at each height we were able to detect velocities as small as $\mathrm{Ca}=5\times10^{-9}$ ($V=0.1$ $\mu$m/s). With this resolution $\Delta\cos\theta=0.60(8)$ for the unetched tube and 0.90(8) for the etched tube. Optical determinations of the range of static contact angles gave consistent values of $\Delta\cos\theta$. For example, the contact line was pinned for angles between 70(5)° and 120(5)° for water-hexadecane in the etched tube.

Theoretical models have produced a range of values for $1/\zeta$. Joanny and Robbins considered the case of a contact line moving past periodic heterogeneities at constant velocity and obtained a result of $1/\zeta=2/3$ for smooth defects [23]. For the case of discontinuous defects they found $\zeta=1$. Raphael and DeGennes independently derived $1/\zeta=2/3$ for smooth defects at dilute concentrations [24]. Functional renormalization group calculations by Ertaş and Kardar yielded $1/\zeta=9/7$ from an expansion around the mean field solution for discontinuous defects ($\zeta=1$) [6]. Sheng and Zhou predicted $0<1/\zeta\leq 0.5$ by considering a capillary wave dissipation mechanism [16].

Experiments have also produced a variety of exponents. The experiment of Stokes *et al.* with a glycerol-methanol solution and mineral oil found that $1/\zeta=0.40(5)$ [18]. Capillary rise experiments showed $1/\zeta=0.5$ for glycerol-water with alkanes as well as for glycerol-water with silicone oils [20]. The difference between our data and the above experiments may be attributable to our use of pure fluids as opposed to mixtures [25]. For mixtures the flow may set up concentration gradients near the interface, leading to a different exponent. Calvo *et al.* in their experiments with the pure fluids water and cyclohexane found logarithmic scaling [19], but their data are not inconsistent with power-law behavior with a small exponent like that found here.

Our experiments indicate that there may be a universal scaling of $\cos\theta$ with Ca for water-alkane interfaces. Further work is needed to extend these results to other fluids and surfaces. The effect of the strongly polar nature of water on the macroscopic behavior of the contact line can be investi-

gated by using a nonpolar fluid as the advancing fluid. The importance of the type of disorder can be evaluated by experiments on substrates silanated to separate the effects of surface structure and chemical disorder, and on surfaces with lithographically patterned surface disorder.

We thank J. P. Stokes and A. P. Kushnick for equipment and advice. This work was supported by the NSF under Grants No. DMR 9357518 and No. DMR 9110004, and by the Exxon Education Foundation. D.H.R. acknowledges support from the David and Lucille Packard Foundation.

[1] P. G. DeGennes, Rev. Mod. Phys. **57**, 827 (1985).
[2] R. G. Cox, J. Fluid Mech. **168**, 169 (1986).
[3] P. A. Thompson and M. O. Robbins, Phys. Rev. Lett. **63**, 766 (1989); P. A. Thompson, W. B. Brinckerhoff, and M. O. Robbins, J. Adhesion Sci. Technol. **7**, 535 (1993).
[4] J. F. Joanny and P. G. DeGennes, J. Chem. Phys. **81**, 552 (1984); Y. Pomeau and J. Vannimus, J. Colloid Interface Sci. **104**, 477 (1985).
[5] M. O. Robbins and J. F. Joanny, Europhys. Lett. **3**, 7577 (1989).
[6] D. Ertaş and M. Kardar, Phys. Rev. E **49**, R2532 (1994).
[7] D. S. Fisher, Phys. Rev. B **31**, 1396 (1985).
[8] G. Blatter, M. V. Feigel'man, V. B. Geshkenbein, A. I. Larkin, and V. M. Vinokur, Rev. Mod. Phys. **66**, 1125 (1994).
[9] N. Martys, M. Cieplak, and M. O. Robbins, Phys. Rev. Lett. **66**, 1058 (1991); Phys. Rev. B **44**, 12 294 (1991).
[10] C. S. Nolle, B. Koiler, N. Martys, and M. O. Robbins, Physica A **205**, 342 (1994).
[11] J. S. Urbach, R. C. Madison, and J. T. Markert, Phys. Rev. Lett. **75**, 276 (1995).
[12] T. Natterman, S. Stepanow, L. H. Tang, and H. Leschhorn, J. Phys. (France) II **2**, 1483 (1992); O. Narayan and D. S. Fisher, Phys. Rev B **48**, 7030 (1993).
[13] H. Leschhorn, Physica A **195**, 324 (1993).
[14] P. Sibani and P. B. Littlewood, Phys. Rev. Lett. **64**, 1305 (1990).
[15] One of the few experimental determinations of $\zeta$ is for charge density wave conduction, S. Bhattacharya, M. J. Higgins, and J. P. Stokes, Phys. Rev. Lett. **63**, 1503 (1989); M. J. Higgins, A. A. Middleton, and S. Bhattacharya, *ibid.* **70**, 3784 (1993).
[16] P. Sheng and M. Zhou, Phys. Rev. A **45**, 5694 (1992).
[17] M. Fermigier and P. Jennfer, J. Colloid Interface Sci. **146**, 226 (1991).
[18] J. P. Stokes, M. J. Higgins, A. P. Kushnick, S. Bhattacharya, and M. O. Robbins, Phys. Rev. Lett. **65**, 1885 (1990).
[19] A. Calvo, I. Paterson, R. Chertkoff, M. Rosen, and J. P. Hulin, J. Colloid Interface Sci. **141**, 384 (1991).
[20] T. A. Mumley, C. J. Radke, and M. C. Williams, J. Colloid Interface Sci. **109**, 413 (1986).
[21] P. K. Dixon and L. Wu, Rev. Sci. Instrum. **60**, 3329 (1989).
[22] E. Charlaix and H. Gayvallet, J. Phys. (France) II **2**, 2025 (1992).
[23] J. F. Joanny and M. O. Robbins, J. Chem. Phys. **92**, 3206 (1990).
[24] E. Raphael and P. G. DeGennes, J. Chem. Phys. **90**, 3206 (1990).
[25] Note that our viscous backgrounds of $2.4\times10^3$ for decane and $4.8\times10^3$ for hexadecane (in the units of Fig. 3) are a much smaller fraction of $P_{ac}^{12}$ than in Ref. [18], and our fits extend over roughly two decades rather than one.